Supramolecular structure of perylene tetracarboxdiimides

V. Marcon[*, 1]**, J. Kirkpatrick**[1, 2]**, W. Pisula**[1]**, and D. Andrienko**[1]

[1] Max-Planck Institute for Polymer Research, Ackermannweg 10, 55128 Mainz, Germany
[2] Department of Physics, Imperial College London, Prince Consort Road, London SW7 2BW, United Kingdom

[*] Corresponding author: e-mail valentina.marcon@mpip-mainz.mpg.de, Phone: +49 6131 379 146, Fax: +49 6131 379 340

Using atomistic molecular dynamics (MD) simulations we study the columnar phases of perylene tetracarboxdiimides (PDI) and establish correlations between the molecular structure, packing, and dynamical properties of these materials.

Combining electronic structure calculations, MD and kinetic Monte Carlo simulations, a correlation is then established between molecular structure and charge mobility of columnar mesophases of perylene tetracarboxdiimide derivatives.

1 Introduction Discotic liquid crystals based on π-conjugated molecules are intensively studied in the field of organic semiconductors. They self-organize into columnar structures both in a solid and liquid crystalline state. Such molecular arrangement allows one-dimensional transport of charge carriers along the well ordered columns, due to the overlap of π-orbitals of neighboring molecules. Discotics have been found suitable for applications in organic field-effect transistors and solar cells [1, 2]. Typical compounds are hexabenzocoronene and triphenylene derivatives, which have been extensively studied both by experimentalists and theoreticians [2, 3].

Most discotics are good hole transporting materials (p-type materials), while only a limited number of good electron transporting ones (n-type materials) have been found [4]. Perylene-diimide (PDI) based compounds have developed into one of the best and widely used n-type semiconductors [5], although *in vacuo* time of flight measurements of mobility yield similar values for hole and electron mobility [26]. Mobilities up to $0.6 \, cm^2 \, V^{-1} \, s^{-1}$ have been reported for thin PDI films [6, 7]. Various PDI derivatives have found application in different areas of organic electronics, such as all-organic photovoltaic solar cells [8–10] and field-effect transistors [5, 11]. Similar to other discotics, self-assembly of PDI derivatives can be controlled by introducing hydrogen bonding [14], metal-ion coordination [15], or by changing the geometry of the side groups [12, 13]. As a result, various supramolecular

structures can be obtained, which have different material properties, in particular charge carrier mobility.

The purpose of this contribution is to establish a correlation between the molecular structure, supramolecular packing and conducting properties of PDI furnished with branched side chains, which is shown in Fig. 1. The synthetic route as well as thermal and structural characterization of the self-organization of this PDI derivative and its higher homologues (terrylene and quaterrylene) has recently been published in Ref. [16]. The mesophase showed a phase transition at 403 K from the crystalline phase directly to the isotropic phase, without an intermediate liquid crystalline state. Based on the data of wide angle X-ray scattering experiments (WAXS) (see Fig. 2), the authors concluded that two molecular arrangements are possible: an orthorhombic lattice with $a = 1.67$ nm and $b = 2.08$ nm or a hexagonal lattice with $a = 4.05$ nm. The meridional reflections were related to the intracolumnar π-stacking with a period of 0.35 nm. The additional meridional reflections corresponding to 1.26 nm were associated with the correlation between every fifth disc in the stack, i.e. a helical packing of molecules in columns with a twist angle between the neighboring molecules of 45 deg. To clarify the experimental observations, we performed molecular dynamics (MD) simulations of columnar mesophases of PDI and used the obtained morphologies to predict the charge mobilities of this system.
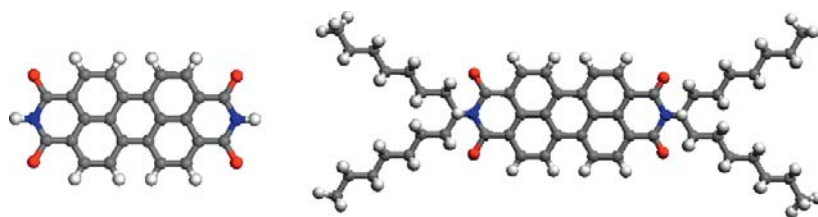
phys. stat. sol. (b) 245, No. 5 (2008)

821

Figure 1 (online colour at: www.pss-b.com) Chemical structure of perylene-diimide (PDI) without (left) and with branched side chains (right). Nitrogens are in blue and oxygens in red.

2 Computational details The simulations were performed with a parallel version of the GROMACS program [17]. The model potential was based on the OPLS all-atom force field [18–20]. A united atom model was used to describe the branched side chains. The parameters of the dihedral and improper terms connecting the perylene core and the side chains, as well as the atomic partial charges, were derived using *ab initio* calculations. The details of these calculations will be published elsewhere.

The simulated systems consisted of 960 perylene molecules, arranged in columns of sixty molecules each. According to the experimental suggestions two different initial lattice configurations were prepared (i) an orthorhombic lattice, simulated at $T = 300$ K (unless otherwise specified) and (ii) a hexagonal lattice, simulated at $T = 400$ K. The choice of the temperatures is based on our previous experience on discotic liquid crystals and the relevant experimental data [18], which showed a better stability of the orthorombic lattice at lower temperatures while the hexagonal configuration was preferred at higher temperatures. After equilibrating the system, production runs of 40 ns with constant pressure, $P = 0.1$ MPa, and constant temperature fixed using the method of Berendsen [21] were performed. Furthermore, in order to check the value of the pitch of the helical structure, several initial configurations with different twist angles and consequently different helical pitches were prepared for both lattices, as shown in Fig. 3.
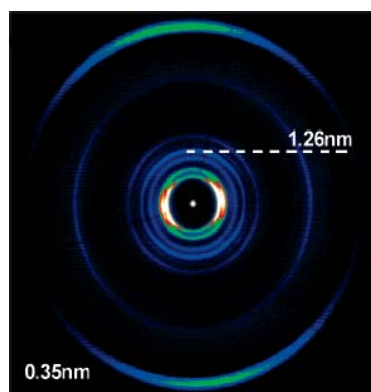

Figure 2 (online colour at: www.pss-b.com) 2D-WAXS patterns of PDI at room temperature. The figure is reproduced from Ref. [16].

3 Results Equilibrated snapshots corresponding to the two different lattices are shown in Fig. 4. The molecules are well-ordered within the columns, with their molecular planes oriented perpendicular to the columnar axes. Small undulations of the columns can be seen, which is due to thermal fluctuations of the director.

To quantify the degree of positional order in the systems, we calculated two distribution functions. The first one, $g_z(r)$, provides information on the distance between molecules in a column. The second one, $g_{xy}(r)$, gives information about the arrangement of the columns with respect to each other. Furthermore, we calculated the orientational order parameter of the columns, Q, which is the largest eigenvalue of the orientational order tensor. $Q = 1$ implies that all the unit vectors perpendicular to the perylene cores are parallel to each other, while $Q = 0$ corresponds to an isotropic distribution of the unit vectors [18].

Both distribution functions are shown in Fig. 5 for a hexagonal lattice and for 45° initial twist angle between the neighbors. Sharp peaks of $g_z(r)$ imply that the molecules are well aligned in the columns; $g_{xy}(r)$ confirms that the columns are arranged on a practically perfect hexagonal lattice. Analyzing the extrema of these distribution functions one can extract a mean separation between the molecules in a column as well as the average distance between the columns. These results are summarized in Tables 1 and 2, for the correspondingly orthorhombic and hexagonal lattices. From this data one can see that the initial configuration has no influence on the distance between molecules in the same column, which is always between 0.35 nm and 0.38 nm, which is in good agreement with experimental data for perylenes and in general for discotic systems based on graphene-type molecules.

Table 1 Orthorhombic lattices at $T = 300$ K. z is the average distance between neighboring molecules along the column, a the lattice parameter, Q the order parameter and ϕ the average twist angle between neighboring molecules.

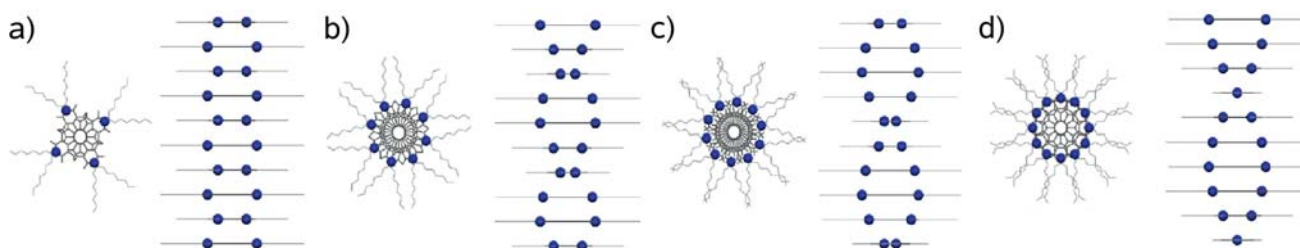|	90°	60°	36°	45°	30°
z (nm)	0.37	0.37	0.36	0.37	0.37
a (nm)	1.86	1.78	1.78	1.62	1.96
Q	0.86	0.90	0.91	0.88	0.84
ϕ (deg)	50.5	55.5	43.9	35.7	35.6

Figure 3 (online colour at: www.pss-b.com) Top and side view of the initial configurations. The twist angle between the neighboring molecules is: a) 90°, b) 45°, c) 36° and d) 30°. Nitrogen atoms are shown in blue.

Table 2 Hexagonal lattices at $T = 400$ K. The same notations are used as in Table 2. Different columns correspond to different initial twist angles.

	90°	60°	36°	45°	30°
z (nm)	0.38	0.37	0.35	0.37	0.37
a (nm)	1.85	1.87	1.91	1.96	1.87
Q	0.86	0.82	0.87	0.73	0.73
ϕ (deg)	44.7	46.6	46.4	39.8	37.0

Table 3 Orthorhombic lattices at different temperatures starting with a twist of 45°.

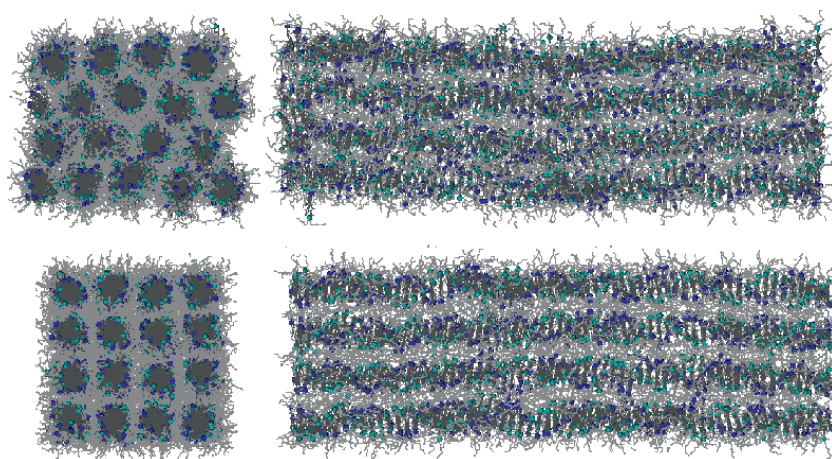|	$T = 300$ K	$T = 400$ K	$T = 450$ K
z (nm)	0.36	0.36	0.36
a (nm)	1.78	1.84	1.89
Q	0.91	0.90	0.86
ϕ (deg)	43.9	43.2	41.0

Figure 4 (online colour at: www.pss-b.com) MD simulation snapshots, hexagonal (top) and orthorhombic (bottom) lattice. On the left are the top views and on the right the side views of the simulation box.
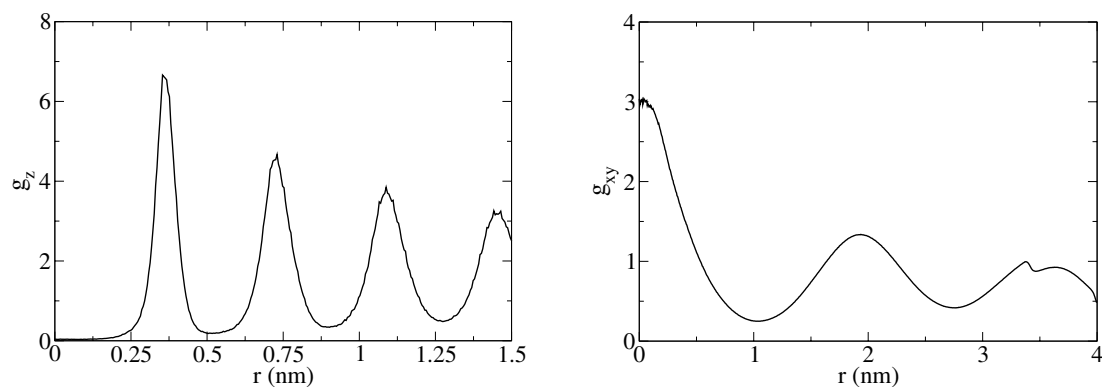

Figure 5 (online colour at: www.pss-b.com) Left: probability of finding another molecule in the same column at a distance r from the reference molecule; right: probability of finding another molecule at a distance r from the reference molecule in the plane perpendicular to the column direction.
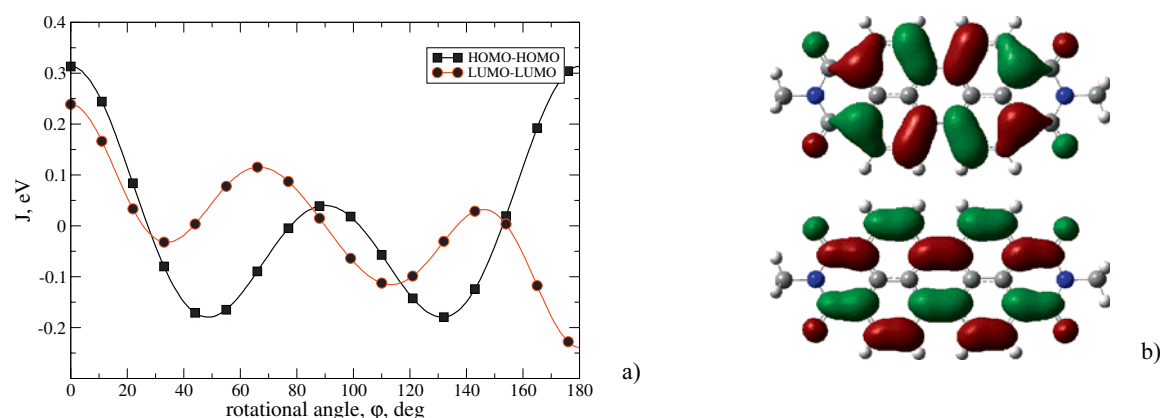
phys. stat. sol. (b) 245, No. 5 (2008)

823

Figure 6 (online colour at: www.pss-b.com) a) Evolution of the transfer integral as a function of the twist angle for holes (HOMO–HOMO) and electrons (LUMO–LUMO). The separation between the molecules was fixed at 3.6 Å, the geometry of a single molecule was optimized using B3LYP hybrid density functional and the 6-311++g(d,p) basis set, while the molecular orbitals were calculated with ZINDO. The transfer integrals were calculated using the molecular orbital overlap method [23]. b) Graphical representation of (top) HOMO and (bottom) LUMO orbitals.

The in-plane arrangement is also not sensitive to the initial value of the pitch, i.e. the systems with an orthorhombic lattice preserve the lattice symmetry during the run. The lattice parameters range from 1.62 nm to 1.96 nm ($a = b$), depending on the initial twist angle. Note that simulations always give a square columnar lattice, while experiments predicts a rectangular one. The lattice constants are, however, very similar.

The hexagonal lattice also preserves its symmetry during the simulation with the lattice parameter a varying between 1.85 nm and 1.96 nm. The parameter provided by experiments, $a = 4.05$ nm, is even larger than that observed for more extended rylenes. This could be explained by the fact the intercolumnar distance is equal to $a = 2.025$ nm, in agreement with simulation data. In fact, such absence of the (100) reflection has already been reported for liquid crystals [22].

In order to understand if one of the two lattices is more stable than the other and if the temperature could bias a phase transition from an orthorhombic to a hexagonal lattice, we simulated the orthorhombic lattice with an initial twist configuration of 45° at two other different temperatures, $T = 400$ K and $T = 450$ K. The results are summarized in Table 3. We find that temperature has no major influence on the structure: even at $T = 450$ K there is no hint of a lattice rearrangement towards the hexagonal arrangement.

The calculated order parameter Q is never lower than 0.73, implying that the alignment of the molecules in columns is always very good. The configurations with an initial twist angle of 45° have the highest value of Q. The better ordering in the orthorhombic lattice is due to the lower temperature ($T = 300$ K) compared to the hexagonal one ($T = 400$ K). This can be also seen from Table 3: the increase of temperature of the orthorhombic lattice corresponds to a decrease of the order parameter, due to a larger movement of the side chains at higher temperature.

To obtain the value of the helical pitch, we calculated an average twist angle between neighboring molecules. The results are summarized in the last line of the tables. They indicate that, independently of the value of the initial twist, all systems reach a final twist angle between 35° and 55°. This confirms the experimental observations of a helix with a pitch of four molecules and an average twist angle of 45°.

Let us now discuss how the helical molecular arrangement can affect the conducting properties of the material. As it has already been mentioned, the transfer integral, which controls the rate of charge transfer between the neighboring molecules, strongly depends on the relative molecular orientations [3]. Its dependence on relative twist is shown in Fig. 6 for electrons and holes. Another parameter which affects charge transfer is the reorganization energy, or electron phonon coupling: a higher reorganization energy will result in slower hopping rates (or narrower bandwidths in the case of band transport [25]). We computed the reorganization energy for electrons and holes following [24] using the B3LYP functional with a triple zeta split basis set (6-311g*). The value of the reorganization energy was computed as 0.25 eV for electrons and 0.14 eV for holes. Since for an angle of 45° the transfer integral for holes is larger than for electrons and since the reorganization energy for holes is smaller than for electrons, we predict that in the columnar mesophase mobilities should be larger for holes. These results suggest that the n-type conduction in PDI is not a function of intrinsic properties but possibly due to exposure to air or difficulty of injecting holes in PDI [26].

4 Outlook The detailed analysis of the structure of perylene tetracarboxdiimides is the starting point to further investigate the microscopic mechanisms of charge carrier mobility. This can be done by combining electronic structure calculations, MD and kinetic Monte Carlo simula-

tions [27]: the transfer integrals are calculated for each pair of neighbors in a column and each MD snapshot. With the knowledge of reorganization energies, one can, using Marcus-Hush theory [28], convert the transfer integrals into the corresponding hopping rates and simulate charge dynamics with numerical techniques such as kinetic Monte Carlo or solution of the Master Equation.

Preliminary results for an orthorhombic lattice with an initial twist of 45° (see Table 3) show that electron mobilities can be as high as 0.21, 0.57, and 0.38 cm^2 V^{-1} s^{-1}, for $T = 300$ K, $T = 400$ K and $T = 450$ K, correspondingly. The calculation of both electron and hole mobilities for all systems, as well as the analysis of their temperature dependence is in progress.

References

[1] F. J. M. Hoeben, P. Jonkheijm, E. W. Meijer, and A. P. H. J. Schenning, Chem. Rev. **105**, 1491 (2005).

[2] J. Wu, W. Pisula, and K. Müllen, Chem. Rev. **107**, 718 (2007).

[3] V. Lemaur, D. A. Da Silva Filho, V. Coropceanu, M. Lehmann, Y. Geerts, J. Piris, M. G. Debije, A. M. Van de Craats, K. Senthilkumar, L. D. A. Siebbeles, J. M. Warman, J.-L. Bredas, and J. Cornil, J. Am. Chem. Soc. **126**, 3271 (2004).

[4] R. J. Chesterfield, J. C. McKeen, C. R. Newmann, P. C. Ewbank, D. A. da Silva Filho, J.-L. Bredas, L. L. Miller, K. R. Mann, and C. D. Frisbie, J. Phys. Chem. B **108**, 19281 (2004).

[5] G. Horowitz, F. Kouki, P. Spearman, D. Fichou, C. Nogues, X. Pan, and F. Garnier, Adv. Mater. **8**, 242 (1996).

[6] W. Struijk, A. B. Sieval, J. E. J. Dakhorst, M. van Dijk, P. Klimkes, R. B. M. Koehorst, H. Donker, T. J. Schaafsma, S. J. Picken, A. M. van de Craats, J. M. Warmann, H. Zuilhof, and E. J. R. J. Sudhölter, J. Am. Chem. Soc. **122**, 11027 (2000).

[7] P. R. L. Malefant, C. D. Dimitrakopoulos, J. D. Gelorme, L. L. Kosbar, T. O. Graham, A. Curioni, and W. Andreoni, Appl. Phys. Lett. **80**, 2517 (2002).

[8] L. Schmidt-Mende, A. Fechtenkötter, K. Müllen, E. Moons, R. H. Friend, and J. D. MacKenzie, Science **293**, 1119 (2001).

[9] J. J. M. Halls and R. H. Friend, Synth. Met. **85**, 1307 (1997).

[10] C. Im, W. Tian, H. Bässler, A. Fechtenkotter, M. D. Watson, and K. Mullen, Synth. Met. **139**, 683 (2003).

[11] B. A. Jones, M. J. Ahrens, M.-H. Yoon, A. Facchetti, T. J. Marks, and M. R. Wasielewski, Angew. Chem. **116**, 6523 (2004).

[12] A. M. van de Craats, J. M. Warman, P. Schlichting, U. Rohr, Y. Geerts, and K. Müllen, Synth. Met. **102**, 1550 (1999).

[13] Z. Chen, V. Stepanenko, V. Dehm, P. Prins, L. D. A. Siebbeles, J. Seibt, P. Marquetand, V. Engel, and F. Würthner, Chemistry **13**, 436 (2007).

[14] X. Zhang, Z. Chen, and F. Würthner, J. Am. Chem. Soc. **129**, 4886 (2007).

[15] F. Würthner, Chem. Commun. **14**, 1564 (2004).

[16] F. Nolde, W. Pisula, S. Müller, C. Kohl, and K. Müllen, Chem. Mater. **18**, 3715 (2006).

[17] E. Lindhal, B. Hess, and D. van der Spoel, J. Mol. Model. **7**, 306 (2001).

[18] D. Andrienko, V. Marcon, and K. Kremer, J. Chem. Phys. **125**, 124902 (2006).

[19] G. Cinacchi, R. Colle, and A. Tani, J. Phys. Chem. B **108**, 7969 (2004).

[20] W. L. Jorgensen, E. R. Laird, T. B. Nguyen, and J. Tirado Rives, J. Comput. Chem. **14**, 206 (1993).

[21] H. J. C. Berendsen, J. P. M. Postma, W. F. van Gunsteren, A. DiNola, and J. R. Haak, J. Chem. Phys. **81**, 3684 (1984).

[22] R. I. Gearba, D. V. Anokhin, A. I. Bondar, W. Bras, M. Jahr, M. Lehmann, and D. A. Ivanov, Adv. Mater. **19**, 815 (2007).

[23] J. Kirkpatrick, Int. J. Quantum Chem., accepted (2007).

[24] M. Malagoli and J. L. Bredas, Chem. Phys. Lett. **327**, 137 (2000).

[25] K. Hannewald, V. M. Stojanovic, J. M. T. Schellekens, P. A. Bobbert, G. Kresse, and J. Hafner, Phys. Rev. B **69**, 075211 (2004).

[26] J. Y. Kim, I. J. Chung, C. Lee, Y. C. Kim, J. K. Kim, and J. W. Yu, Curr. Appl. Phys. **5**, 615 (2004).

[27] J. Kirkpatrick, V. Marcon, J. Nelson, K. Kremer, and D. Andrienko, Phys. Rev. Lett. **98**, 227402 (2007).

[28] K. F. Freed and J. Jortner, J. Chem. Phys. **52**, 6272 (1970).